

# A Beamformer-Particle Filter Framework for Localization of Correlated EEG Sources

Petia Georgieva, *Senior Member, IEEE*, Nidhal Bouaynaya, *Member, IEEE*, Filipe Silva, *Member, IEEE*, Lyudmila Mihaylova, *Senior Member, IEEE*, and Lakhmi Jain

**Abstract**—Electroencephalography (EEG)-based brain computer interface (BCI) is the most studied non-invasive interface to build a direct communication pathway between the brain and an external device. However, correlated noises in EEG measurements still constitute a significant challenge. Alternatively, building BCIs based on filtered brain activity source signals instead of using their surface projections, obtained from the noisy EEG signals, is a promising and not well explored direction. In this context, finding the locations and waveforms of inner brain sources represents a crucial task for advancing source-based non-invasive BCI technologies. In this paper, we propose a novel Multi-core Beamformer Particle Filter (Multi-core BPF) to estimate the EEG brain source spatial locations and their corresponding waveforms. In contrast to conventional (single-core) Beamforming spatial filters, the developed Multi-core BPF considers explicitly temporal correlation among the estimated brain sources by suppressing activation from regions with interfering coherent sources. The hybrid Multi-core BPF brings together the advantages of both deterministic and Bayesian inverse problem algorithms in order to improve the estimation accuracy. It solves the brain activity localization problem without prior information about approximate areas of source locations. Moreover, the multi-core BPF reduces the dimensionality of the problem to half compared with the PF solution; thus alleviating the curse of dimensionality problem. The results, based on generated and real EEG data, show that the proposed framework recovers correctly the dominant sources of brain activity.

**Index Terms**—EEG inverse problem, spatial-temporal brain source localization, Bayesian estimation, particle filtering, multi-core beamformer

## I. INTRODUCTION

**E**lectroencephalography (EEG) is a widely used technology for brain study because it is non-invasive, relatively cheap, portable and with an excellent temporal resolution. These salient features hold the promise of EEG-based Brain Computer Interface (BCI) technologies [1] capable of building alternative communication channels between humans and the external world. The spatial-temporal reconstruction of the underlying brain neural generators based on the EEG recording has emerged as an active area of research over the last decade. Several source reconstruction approaches, each employing a different set of assumptions, have been proposed to overcome

the ill-posed inverse problem. They can be divided in two main classes, [2]: *i*) imaging models (also known as current density reconstruction models), which explain the data with a dense set of current dipoles distributed at fixed locations; and *ii*) equivalent current dipole models (also known as point source or parametric models), which assume a small number of focal sources at locations to be estimated from the data.

While the imaging techniques provide a detailed map of the neuronal activity, the parametric models represent a direct mapping from scalp topology to a small number of parameters. Dipole solutions provide more intuitive interpretations that explain the sensor data. Furthermore, it is easy to report statistics of dipole parameters over different subjects. Summarizing distributed brain activity with a small number of active dipoles simplifies the analysis of connectivity among those sources. Additionally, building BCIs based on the neuronal sources instead of the EEG sensor data is gaining more interest [3]–[6]. In particular, source-based BCI seems an appealing alternative to well known invasive solutions through implant placement (intra-cortical electrodes) by neurosurgery.

Popular deterministic parametric solutions include the Multiple Signal Classification (MUSIC) algorithm and its modified versions [7], the methods for inverse problems [8], the construction of spatial filters by data-independent [9] or data-driven methods [10] and blind source separation techniques [11], [12]. However, these approaches are based on the assumption that the brain source locations are known a priori or perform a search of the overall head volume to find their positions. Given the spatial source locations, they estimate the amplitudes and directions of the source waveforms.

Recently, statistical methods have gained popularity. Galka et al. [2] consider the inverse problem as a dynamical one and apply Kalman filtering to a linear distributed EEG source model. In Kiebel et al. [13] a variational Bayesian approach is developed, which allows for specification of priors on all the model parameters. Following a similar approach as [2], Sorrentino et al. [14], [15] propose a dynamical Bayesian framework to estimate the locations of magnetoencephalographic (MEG) sources.

In the statistical state-space model framework, the EEG source localization problem is formulated as the estimation of the posterior probability density function (pdf) of the state based on the available observations. For the linear and Gaussian estimation problem, the Kalman filter propagates and updates the mean and covariance of the distribution. For non-linear problems and non-Gaussian noise, there is no general analytical solution to the posterior density estimation problem.

P. Georgieva and F. Silva with the Institute of Electronics Engineering and Telematics of Aveiro, Department of Electronics, Telecommunications and Informatics, University of Aveiro, 3810-193 Aveiro, Portugal (e-mail: petia@ua.pt; fmsilva@ua.pt), N. Bouaynaya is with the Department Electrical and Computer Engineering, Rowan University, Glassboro, NJ, USA (e-mail: bouaynaya@rowan.edu), L. Mihaylova (corresponding author) is with the Department of Automatic Control and Systems Engineering, University of Sheffield, United Kingdom (e-mail: l.s.mihaylova@sheffield.ac.uk), L. Jain is with the University of South Australia, Australia (e-mail: lakhmi.jain@unisa.edu.au)

Therefore, a numerical approach is needed to evaluate the posterior pdf of the state vector. The Particle Filter [16], [17] has emerged, within the object tracking community, as one of the most successful methods for state estimation in highly non-linear or non-Gaussian state-space models. The main idea is to represent the posterior pdf as a set of random samples, called particles. When propagated and weighted properly, these samples tend to the exact pdf as the number of samples becomes very large [17]. The recent surveys [17]–[20] show successful applications of particle filtering to different areas.

The computational complexity is a major challenge in the reviewed techniques for brain source analysis. It is related with the number of estimated dipoles, the dimension of the dipole grid over which the active dipoles are searched and the dipole temporal correlation. Deterministic solutions like the MUSIC algorithm and its variations look for a trade-off between the dense dipole grid space and correct dipole estimation of an unlimited number of uncorrelated dipoles, or large grid spacing (for fast computation), but sources may be missed or incorrectly estimated if their true location is too far apart from a grid point. Spatial filters like Beamforming (BF) have the advantage of providing closed-form linear solution of the inverse problem [21], [22]. However, they are rather sensitive to correlated dipoles and require knowledge of the dipole positions. Statistical approaches, like particle filtering, are more suitable to the brain source analysis but they have to deal with the problem of the high state vector dimension that usually deteriorates the estimation accuracy. For example, in a full particle filter framework, one estimated dipole corresponds to 6 estimated parameters (3 space location coordinates and 3 directions of dipole moments propagation). This problem is addressed in [23] by an algorithm that integrates multiple particle filters to estimate individual dipoles. However, such a framework does not provide tools for analyzing a potential dipole correlation and connectivity, which is a central issue in neuroscience. Moreover, applying a full particle filter, designed for solving nonlinear problems, for estimation of dipole moments, a linear function of the EEG signal, is an unjustified complication of the inverse problem.

In order to overcome the limitation of the conventional (single-core) BF [10], [24] to reconstruct only uncorrelated sources, Brookes et. al. [25] and Diwakar et al. [26] proposed a dual-core BF to consider two simultaneously activated sources into a single spatial filter. Dalal et al [27] and Popescu [28] extended the methodology of Diwakar, by adding multiple null-constraints in the potentially correlated source locations (multi-core Beamformer). A combined solution of the brain dipole recovery is proposed in [29], referred to as a Beamforming Particle Filter (BPF), where a single-core BF is used to estimate the source waveforms and a particle filter (PF) to estimate the source spatial locations. The algorithm was illustrated for one dipole.

The key contributions of this work are the following: 1) We propose a hybrid approach (multi-core BF and PF) that, in contrast to previous solutions, does not assume knowledge of the spatial locations of the brain sources in order to estimate the waveforms. The spatial dipole coordinates are estimated using the PF, whereas the waveforms are estimated

using the Beamformer; 2) The multi-core BF reconstructs the moments of each identified dominant source considering null constraints with respect to the others. Since the number of the identified sources (by PF) is smaller than the suppressed single correlated interferers or nulling entire brain volumes as in previous works [27], [28], the computational complexity of the proposed combined solution is significantly lower.;3) Satisfactory reconstruction accuracy was obtained for very low EEG Signal to Noise Ratios (less than 8 dB) which is an additional advantage of the hybrid approach.

This paper is organized as follows: In Section II the PF framework is outlined. Section III presents the EEG state-space model in order to apply the PF, based on physiological specifications. The Beamformer for correlated sources is introduced in Section IV. The joint Multi-core Beamformer and Particle Filter (Multi-core BPF), for recursive estimation of the source locations and waveforms is presented in Section V. In Section VI, the Multi-core BPF is applied to simulated and real EEG data and compared with alternative solutions. Section VII summarizes the results.

## II. THE PARTICLE FILTER

The active zones in the brain can be described in general with a nonlinear state space model defined by the state and measurement equations:

$$\mathbf{x}_{k+1} = \mathbf{f}_k(\mathbf{x}_k, \mathbf{w}_k) \quad (1)$$

$$\mathbf{z}_k = \mathbf{h}_k(\mathbf{x}_k, \mathbf{v}_k), \quad (2)$$

where  $f_k$  is the system transition function and  $\mathbf{w}_k$  is a zero-mean, white noise sequence of known pdf, independent of past and current states and  $k$  is the discrete time index. Measurements  $\mathbf{z}_k$ ,  $k = 1, 2, \dots$ , are available at discrete time steps  $k$ , relating to the unknown state vector  $\mathbf{x}_k$  via the observation equation in (2), where  $h_k$  is the measurement function and  $\mathbf{v}_k$  is a zero-mean, white noise sequence of known pdf, independent of past and present states and the system noise.

Within the Bayesian framework, all relevant information about the state vector, given observations  $\mathbf{Z}_{1:k} = \{\mathbf{z}_1, \dots, \mathbf{z}_k\}$  up to and including time  $k$ , can be obtained from the posterior distribution of the state  $p(\mathbf{x}_k | \mathbf{Z}_{1:k})$ . This distribution can be obtained recursively in two steps: prediction and update. Suppose that the posterior distribution at the previous time index  $k-1$ ,  $p(\mathbf{x}_{k-1} | \mathbf{Z}_{1:k-1})$ , is available. Then, using the system transition model, we can obtain the prior pdf of the state at time  $k$  as follows:

$$p(\mathbf{x}_k | \mathbf{Z}_{1:k-1}) = \int p(\mathbf{x}_k | \mathbf{x}_{k-1}) p(\mathbf{x}_{k-1} | \mathbf{Z}_{1:k-1}) d\mathbf{x}_{k-1}. \quad (3)$$

When a measurement, at time step  $k$ , is available, the prior is updated via the Bayes rule [30], [31]:

$$p(\mathbf{x}_k | \mathbf{Z}_{1:k}) = \frac{p(\mathbf{z}_k | \mathbf{x}_k) p(\mathbf{x}_k | \mathbf{Z}_{1:k-1})}{p(\mathbf{z}_k | \mathbf{Z}_{1:k-1})}, \quad (4)$$

where the denominator is a normalizing factor and the conditional pdf of  $\mathbf{z}_k$  given  $\mathbf{x}_k$  is defined by the measurement model in (2).

The recursive equations in (3) and (4) constitute the solution to the Bayesian estimation problem. If the functions  $f_k$  and

$h_k$  are linear and the noises  $w_k$  and  $v_k$  are Gaussian with known variances, then an analytical solution to the Bayesian recursive estimation problem is given by the well-known Kalman filter [32]. In the EEG source localization problem, however, the measurement function  $h_k$  is non-linear, i.e. the EEG measurements  $z_k$  are non-linear functions of the source locations  $x_k$  [33]. The measurement model will be presented in the sequel.

In order to deal with the non-linear models and/or non-Gaussian noises, two main approaches have been adopted: parametric and non-parametric. The parametric techniques are based on extensions of the Kalman filter by linearizing non-linear functions around the predicted values [34]. Other Kalman filter variants such as the Extended Kalman filter and Unscented Kalman filter [35] exist but they can only deal with unimodal distributions. Because of their first-order approximations and unimodal Gaussian assumptions, such extensions find difficulties in dealing with multi-model distributions. Non-parametric methods such as Monte Carlo methods [16], [30], [35] use a set of random samples, called particles, to represent the posterior pdf. The posterior is then approximated by a set of weighted particles (hence the name particle filter) as [16]:

$$p(\mathbf{x}_k | \mathbf{Z}_{1:k}) \approx \sum_{i=1}^N \pi_k^{(i)} \delta(\mathbf{x}_k - \mathbf{x}_k^{(i)}), \quad (5)$$

where  $N$  is the total number of particles,  $\pi_k^{(l)} = \frac{w_k^{(l)}}{\sum_{l=1}^N w_k^{(l)}}$  is the normalized weight for particle  $l$  at time  $k$  and  $\delta(\cdot)$  is the Dirac delta function.

Different methods [19], [20], [35] have been proposed to update the current weights  $w_k^{(l)}$  based on previous weights  $w_{k-1}^{(l)}$  and measurement  $z_k$ . Sampling-importance-resampling (SIR) is the most popular method where the importance weight of a particle is given by [16], [30], [35]:

$$w_k^{(l)} = w_{k-1}^{(l)} \frac{p(z_k | \mathbf{x}_k^{(l)}) p(\mathbf{x}_k^{(l)} | \mathbf{x}_{k-1}^{(l)})}{q(\mathbf{x}_k^{(l)} | \mathbf{x}_{k-1}^{(l)}, \mathbf{Z}_{1:k})}, \quad (6)$$

where  $q(\mathbf{x}_k^{(l)} | \mathbf{x}_{k-1}^{(l)}, \mathbf{Z}_{1:k})$  denotes the importance function from which samples are drawn. The most popular choice [16] for the prior importance function is  $q(\mathbf{x}_k^{(l)} | \mathbf{x}_{k-1}^{(l)}, \mathbf{Z}_{1:k}) = p(\mathbf{x}_k^{(l)} | \mathbf{x}_{k-1}^{(l)})$  and it implies that equation (6) reduces to:

$$w_k^{(l)} = w_{k-1}^{(l)} p(z_k | \mathbf{x}_k^{(l)}). \quad (7)$$

Given a discrete approximation to the posterior distribution, one can then proceed to a filtered point estimate such as the mean of the state at time  $k$ :

$$\hat{\mathbf{x}}_k = \sum_{l=1}^N \pi_k^{(l)} \mathbf{x}_k^{(l)}. \quad (8)$$

The main advantage of the particle filter is that no restrictions are placed on the modeling functions  $f_k$  and  $h_k$ , or on the distribution of the system and measurement noise. Moreover, the algorithm is quite simple and very easy to implement. However, this increases the computational cost. Notably, it can be implemented on massively parallel computers, raising the possibility of real time operation with very large sample sets.

### III. THE EEG STATE-SPACE MODEL

In order to apply the particle filtering framework, we need to define the state-space model of the EEG source localization problem based on physiological constraints. The state vector  $\mathbf{x}_k$ , at time  $k$ , represents the coordinates of the brain sources, or dipoles, within the three-dimensional head geometry. For example, for two dipoles, the state vector comprises  $(x_{ik}, y_{ik}, z_{ik})$ , the three dimensional coordinates of the  $i^{th}$  dipole in the chosen head geometry at time  $k$ ,  $\mathbf{x}_k = [x_{1k}, y_{1k}, z_{1k}, x_{2k}, y_{2k}, z_{2k}]^t$  and  $t$  is the transpose operator. The observation vector  $\mathbf{z}_k$  represents the EEG measurements collected from all sensors at time  $k$ . The goal is to estimate the brain source locations given the multichannel EEG signal.

#### A. The EEG Measurement Model

The main source of EEG potentials, measured at the scalp, derive from simultaneous postsynaptic current flows of many neighboring neurons with similar orientations. In particular, these clusters of similar oriented neurons are mainly found in the cortical areas of the brain associated with the pyramidal cells. The total electric current in an activated region is often modelled by a mathematical current dipole with an adequate dipole moment. Additionally, many of those current dipoles representing microscopic current flows with the same orientation can be replaced by an equivalent current dipole [1]. Assuming that the electrical activity of the brain is originated from  $M$  dipolar sources, the measured multichannel EEG signal  $\mathbf{z}_k$  from  $n_z$  sensors at time  $k$  can be expressed by:

$$\mathbf{z}_k = \sum_{m=1}^M \mathbf{L}_m(\mathbf{x}_k(m)) \mathbf{s}_k(m) + \mathbf{v}_k, \quad (9)$$

where  $\mathbf{x}_k(m)$  is a  $3M \times 1$ -dimensional state vector, that represents the spatial source location at time  $k$ ,  $\mathbf{L}_m(\mathbf{x}_k(m))$  is the  $n_z \times 3$  leadfield matrix, also called forward matrix, for the  $m^{th}$  dipole;  $\mathbf{s}_k(m)$  is a  $3 \times 1$ -dimensional moment of the  $m^{th}$  dipole at time  $k$ , and  $\mathbf{v}_k$  is a white Gaussian model noise with covariance  $\mathbf{C}_v$ . The components of the leadfield matrix  $\mathbf{L}_m$  are non-linear functions of the dipole localization, electrodes' positions and head geometry [33]. Note also, from equation (9), that the EEG measurements  $\mathbf{z}_k$  are linear with respect to the dipole moments  $\mathbf{s}_k$  and non-linear with respect to their spatial locations  $\mathbf{x}_k$ . Though we are assuming that the number of dipoles  $M$  is known, it can be estimated by analysing the structure of the covariance matrix of the observations and using information-theoretic criteria, as presented in [36].

Equation (9), which takes into account  $M$  dipoles, can be written in the following concise form:

$$\mathbf{z}_k = \mathbf{L}(\mathbf{x}_k) \mathbf{s}_k + \mathbf{v}_k, \quad (10)$$

where  $\mathbf{x}_k = [\mathbf{x}_k(1), \dots, \mathbf{x}_k(M)]^t$  is a  $3M \times 1$  vector, representing the 3D location coordinates of the  $M$  dipoles at time  $k$ ,  $\mathbf{L}(\mathbf{x}_k) = [\mathbf{L}_1(\mathbf{x}_k(1), \dots, \mathbf{L}_M(\mathbf{x}_k(M))]$  is a  $n_z \times 3M$  lead field matrix of the  $M$  dipoles at time  $k$ , and  $\mathbf{s}_k = [\mathbf{s}_k(1), \dots, \mathbf{s}_k(M)]$  is the  $3M \times 1$  vector of brain source signals in the three directions for the  $M$  dipoles. From Eq.

(10), we can compute the likelihood of each measurement as:

$$\mathcal{L}(\mathbf{z}_k | (\mathbf{x}_k, \mathbf{s}_k)) \propto \exp \left[ -\frac{(\mathbf{z}_k - \mathbf{L}(\mathbf{x}_k)\mathbf{s}_k)^t \mathbf{C}_v^{-1} (\mathbf{z}_k - \mathbf{L}(\mathbf{x}_k)\mathbf{s}_k)}{2} \right], \quad (11)$$

where  $\propto$  denotes ‘‘proportional to’’.

### B. The EEG State Transition Model

We assume no a priori knowledge of the source locations. This is in contrast to other studies where a prior information may be available from other brain imaging modalities like Magneto resonance Images (MRI) or functional MRI. We therefore, assume the state transition to be a random walk (first-order Markov chain) in the source localization space:

$$\mathbf{x}_k = \mathbf{x}_{k-1} + \mathbf{w}_k, \quad (12)$$

where  $\mathbf{w}_k$  is a zero-mean, Gaussian white noise sequence with covariance  $\sigma_w^2 \mathbf{I}$ . The process  $\mathbf{w}_k$  is assumed to be independent of past and current states. The Gaussianity of the system and measurement noise is justified by the Central Limit Theorem, because of the numerous sources of noise introduced in EEG measurements: (i) environmental noise, which comes from the power line and bad electrode contacts; (ii) physiological noise, which arises from artifacts like the heart rate or eye blinks; and (iii) background noise, which is the result of the constant brain activity.

The state-space model of the dipole source localization problem is then given by:

$$\begin{cases} \mathbf{x}_k = \mathbf{x}_{k-1} + \mathbf{w}_k, & \text{state transition model} \\ \mathbf{z}_k = \mathbf{L}(\mathbf{x}_k)\mathbf{s}_k + \mathbf{v}_k, & \text{observation model.} \end{cases} \quad (13)$$

In the above model, the source waveforms  $\mathbf{s}_k$  are not known and they are estimated by the beamforming filter.

## IV. MULTI-CORE BEAMFORMING FOR CORRELATED SOURCE LOCALISATION

The Beamforming (BF), originated in radar and sonar field, is a well-known spatial filter for EEG source estimation [24], [37]–[43]. The BF estimates the source moments  $\mathbf{s}_k$  by applying the following linear operator:

$$\mathbf{s}_k = \mathbf{W}^t \mathbf{z}_k, \quad (14)$$

where  $\mathbf{W}^t$  is an  $n_z \times 3M$  weighting matrix. The ideal filter transmits the signals from the location of interest with a unit gain, while nulling signals from elsewhere (i.e., insensitive to the activity from other brain regions). Among a number of criteria for choosing the optimal matrix  $\mathbf{W}$ , the eigenspace-projected linearly constrained minimum variance (LCMV) BF gained much interest [39], [44]. The LCMV formulation allocates spatial nulls so as to minimize the contribution to the filter output from sources at locations other than the estimated source [28]. Under the assumption that source moments associated with different sources are temporally uncorrelated, the solution to this minimization problem is given by [10]

$$\begin{aligned} \mathbf{W}^* &= \underset{\mathbf{W}}{\operatorname{argmin}} \operatorname{Tr} [\mathbf{W}^t \mathbf{C}_v \mathbf{W}] \\ &\text{subject to } \mathbf{W}^t \mathbf{L}(\mathbf{x}_k) = \mathbf{I}. \end{aligned} \quad (15)$$

The optimal solution is derived by constrained minimization using Lagrange multipliers,

$$\mathbf{W}^* = \mathbf{C}_v^{-1} \mathbf{L}(\mathbf{x}_k) [\mathbf{L}(\mathbf{x}_k)^t \mathbf{C}_v^{-1} \mathbf{L}(\mathbf{x}_k)]^{-1}. \quad (16)$$

The conventional (single-core) LCMV Beamformer, described above, has an important limitation when spatially distinct yet temporally correlated sources are present in the EEG signal [10], [24]. Its main assumption is that the activity at the target location is not linearly correlated with activity at any other location. However, several studies of functional connectivity have suggested that temporal correlation relates to the communications among cortical areas. For example, such high correlations occur during evoked sensory responses in which the sensory information is transmitted to both left and right auditory cortices simultaneously, which result in almost perfectly correlated activities in the two hemispheres [41]. Correlated activities can also be observed in symmetric regions of the left and right hemispheres of the motor cortex [45], [46].

Different modifications of the single-core BF attempt to compensate for this limitation. The temporal correlation  $M_{i,j}(f)$  of a pair of  $(i, j)$  dipoles is quantified by the magnitude-squared cross spectrum  $S_{i,j}(f)$  divided by the power spectra of both dipole moments  $S_{i,i}(f)$  and  $S_{j,j}(f)$ :

$$M_{i,j}(f) = \frac{|S_{i,j}(f)|^2}{S_{i,i}(f)S_{j,j}(f)}. \quad (17)$$

The correlation is bounded between 0 and 1, where  $M_{i,j}(f) = 1$  indicates a perfect linear relation between dipoles  $d_i$  and  $d_j$  at frequency  $f$ .

Dynamic imaging of coherent sources (DICS) is proposed in [9] where the spatial filter weighting matrix explicitly takes into account the estimated correlation quantified by equation (17). The authors of [47] conclude that high coherence results in a large error in the estimation of the dipole location. Low SNR additionally deteriorates the estimation of spatially close and temporally correlated dipoles. Correlated dipoles can be reliably localized if the distance between them is sufficiently high. DICS computes the cross spectral densities for any given location (from a dense grid of points) and all pair combinations of grid dipoles.

Inspired by the methodology of Diwakar et al. [26] we have developed an adaptive beamformer based on the LCMV algorithm with multiple constraints in the potentially correlated source locations. The optimization problem is solved using the method of Lagrange multipliers with multiple constraints:

$$\begin{aligned} \min_{\mathbf{W}} \quad & \operatorname{Tr} [\mathbf{W}^t \mathbf{C}_v \mathbf{W}] \\ \text{subject to} \quad & \mathbf{W}^t \mathbf{L}(\mathbf{d}_1) = \mathbf{I}. \\ & \mathbf{W}^t \mathbf{L}(\mathbf{d}_2) = \mathbf{0}. \\ & \vdots \\ & \mathbf{W}^t \mathbf{L}(\mathbf{d}_M) = \mathbf{0}. \end{aligned} \quad (18)$$

The conventional beamformer (BF) is characterized with high computational costs due to the scanning solution over a 3D source grid with thousands of nodes (potential source locations). The BF modifications to account for correlated sources increase even more the computational burden because of the additional cross correlation estimation for all pair combinations of grid dipoles. Moreover, the limited number

of EEG channels restricts the degree of freedom and limits the number of constrains that can be considered.

We propose to deal with this problem by the iterative multi-core BF-PF procedure where starting from randomly generated assumption for the dipole spatial coordinates of the active dipoles (uninformed prior) the PF converges to a small number of dominant sources. The multi-core BF reconstructs the moments of each identified dominant source considering null constrains with respect to the others identified by the PF. The advantage of this combined solution is that the number of constrains in (18) is kept low and no a priori information for the expected spatial localization of the correlated sources is required. We rely on the estimation properties of the PF to converge to the actual active dipoles.

## V. THE MULTI-CORE BEAMFORMER-BASED PARTICLE FILTER

The Multi-core Beamformer Particle Filter (Multi-core BPF) is a hybrid (statistical-deterministic) framework for reconstruction of correlated source. The PF provides estimates of the location of fixed temporally correlated brain sources in a three dimensional space within the head defined by a grid of points. The ability to simultaneously and recursively estimate the source locations and waveforms lies in the BF spatial filter that is embedded within the particle filter framework to estimate the dipole moments for a given PF estimation of the dipole location. The Multi-core BPF algorithm is summarized below.

---

### Multi-core Beamformer Particle Filter for Correlated Source Localization

---

#### 1) Offline computation

Compute and store the forward matrices  $\mathbf{L}$  for all points of the grid by solving the Maxwell equations in [33].

#### 2) Initialization

- a)  $k = 0$ , for  $l = 1, \dots, N$ , where  $N$  denotes the total number of particles, generate samples  $\mathbf{x}_0^{(l)} \sim p(\mathbf{x}_0)$  and set initial weights  $\pi_0^{(l)} = 1/N$ .
- b) for  $k = 1, 2, \dots$

#### 3) Prediction step

for  $l = 1, \dots, N$ , generate samples according to the state transition model in Eq. (12):

$$\mathbf{x}_k^{(l)} = \mathbf{x}_{k-1}^{(l)} + \mathbf{w}_k^{(l)}, \text{ where } \mathbf{w}_k^{(l)} \sim \mathcal{N}(\mathbf{0}, \sigma_w^2 \mathbf{I}) \quad (19)$$

#### 4) Multi-core Beamforming

- a) Find the lead field matrix  $\mathbf{L}(\mathbf{x}_k^{(l)})$  for each predicted dipole from the offline calculation.
- b) Find the optimal spatial filter weights using (18). Consider the location of each estimated dipole  $d_i (i = 1, \dots, M)$  as the targeted direction and the other  $M - 1$  dipoles as correlated with  $d_i$  to compute the weighted vector associated with it.
- c) Compute the source waveforms  $\mathbf{s}_k^{(l)}$  according to (14).

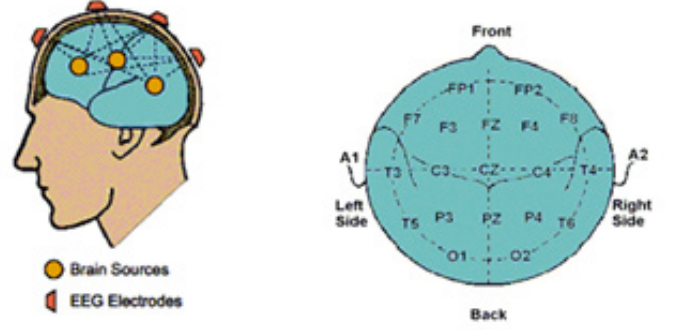


Fig. 1. The head model: (a) depiction of a realistic EEG experiment (left); (b) spatial scalp location of the EEG electrodes (right).

#### 5) Measurement update

Evaluate the particle weights

- a) for  $l = 1, 2, \dots, N$ , on the receipt of a new measurement, compute the weights
$$w_k^{(l)} = w_{k-1}^{(l)} \mathcal{L} \left( z_k \mid \left( \mathbf{x}_k^{(l)}, \mathbf{L}(\mathbf{x}_k^{(l)}), \mathbf{s}_k^{(l)} \right) \right). \quad (20)$$

The likelihood  $\mathcal{L} \left( z_k \mid \left( \mathbf{x}_k^{(l)}, \mathbf{L}(\mathbf{x}_k^{(l)}), \mathbf{s}_k^{(l)} \right) \right)$  is calculated using (11).

- b) for  $l = 1, 2, \dots, N$ , normalize the weights,

$$\pi_k^{(l)} = w_k^{(l)} / \sum_{l=1}^N w_k^{(l)}. \quad (21)$$

- 6) Evaluate the posterior mean as the estimate of the state at iteration  $k$

$$\hat{\mathbf{x}}_k = E[\mathbf{x}_k \mid \mathbf{Z}_{1:k}] = \sum_{l=1}^N \pi_k^{(l)} \mathbf{x}_k^{(l)}. \quad (22)$$

- 7) Compute the effective sample size  $N_{eff} = 1 / \sum_{l=1}^N (\pi_k^{(l)})^2$ .

- 8) Selection step (resampling) if  $N_{eff} < N_{thresh}$ : multiply/suppress samples  $\{\mathbf{x}_k^{(l)}\}$  with high/low weights  $\pi_k^{(l)}$ , in order to obtain  $N$  new random samples approximately distributed according to the posterior state distribution.

---

Resampling is performed when the efficient number of particles  $N_{eff}$  is below a fixed threshold  $N_{thresh}$ .

## VI. SIMULATION RESULTS

The performance of the proposed approach is assessed by simulation experiments assuming the EEG signals are generated by a limited number of focal sources. A three-shell spherical head model (Figure 1) was created based on the following assumptions:

- The head model consists of three concentric spherical shells with the enclosed space among them representing the scalp, skull and brain. The model dimensions are scaled to a realistic human head with an outer shell radius of 10 cm, scalp radius of 9.2 cm and skull radius of 8.7 cm.

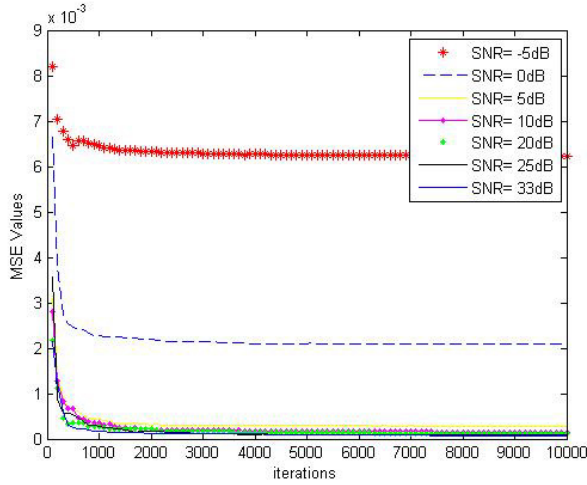


Fig. 2. Robustness of the proposed beamformer-based particle filter under varying SNR.

- Each layer is considered as homogeneous and isotropic, i.e., conductivity is constant and with no preferred direction. The conductivity values used for the head model were selected from studies on electrical impedance tomography (EIT) aiming to create an electrical conductivity map of a volume [48]: scalp 0.33 S/m, skull 0.0165 S/m and brain 0.33 S/m.
- The distribution of the electrodes on the scalp follows the standard 10/20 International system with an array of 30-electrodes: Fp1, AF3, F7, F3, FC1, FC5, C3, CP1, CP5, P7, P3, Pz, PO3, O1, Oz, O2, PO4, P4, P8, CP6, CP2, C4, FC6, FC2, F4, F8, AF4, Fp2, Fz, Cz.
- The coordinates are defined with respect to a reference frame whose origin is located at the centre of the sphere: the  $x$ -axis pointing in the direction of the right-ear, the  $y$ -axis pointing in the front of the head and the  $z$ -axis is taken to be vertical.

White noise was added into the generated EEG signals representing the effect of external sources not generated by brain activity, but by some disturbance (e.g., movements of muscles). The noise power was defined for different signal-to-noise ratios (SNR). The SNR is defined in the sensor domain as the total power of the signal divided by the total power of the noise added to the signal. The total searchable head volume is simulated with a fixed uniform grid model of 21012 points (potential dipoles). The leadfield matrix is computed off-line for each grid dipole. The experiments were done on a PC Intel Core with CPU 2 GHz, RAM 8GB, 64 bit OS, Windows 8.1.

#### A. Dipole Localization Results

Sinusoidal waveforms with amplitudes 0.1 and frequencies 10 Hz and 15 Hz are assumed to be the brain signals originating from the two dipoles ( $d_1$  and  $d_2$ ). Observe that the dimension of the state vector  $\mathbf{x}_k = [x_{1k}, y_{1k}, z_{1k}, x_{2k}, y_{2k}, z_{2k}]^t$  is 6, corresponding to three space coordinates per dipole. For the initial state vector,  $N=500$  samples are randomly generated from a uniform distribution in the interval  $\mathbf{x}_0 \in$

$[\min(D), \max(D)]$  with  $D$  is the coordinates of a grid of dipoles, i.e.,  $D = \{d_i = [x_i, y_i, z_i]\}$ .

The PF finds the brain source coordinates  $\mathbf{x}_k$  within the head geometry as presented in Figure 1.

In the simulations, the sources are randomly generated and, therefore, they may or may not coincide with the dipole grid that describes the head model. We consider three cases: (i) the two brain sources are located on the dipole grid; (ii) only one brain source coincides with a dipole grid, and (iii) none of the brain sources is located on the dipole grid. Figures 3, 4 and 5 show the absolute estimation error for the three cases with all simulations running for 200 iterations or time points. For display quality, we only show the first iterations after which the algorithm converges. We observe that the absolute estimation errors with respect to the space coordinates  $(x, y, z)$  converge almost to zero after 10 iterations if the original brain sources are located on the grid head model. The ground truth dipoles are  $d_1 : (0.0116, 0.0767, 0.019)m$  and  $d_2 : (-0.0116, -0.0767, 0.0095)m$ .

The estimation of the locations of non-grid-dipoles ends with a small steady-state error. The ground truth dipoles are now close but do not coincide with any grid point  $d_1 : (0.01, 0.075, 0.02)m$  and  $d_2 : (-0.01, -0.075, -0.01)m$ . This error can be reduced if the grid model is more dense. However, including very closely spaced sources lead to ill-conditioned null-constraints in [28], [49]. It is worth pointing out that in Figs. 3-5 the differences in the convergence behavior between the two dipoles are mainly due to the small number of particles ( $N = 500$ ). If the number of particles increases enough, the convergence behavior of the two dipoles (in every scenario) would be statistically similar.

The robustness of the proposed Multi-core BPF to the noise in the EEG dataset was also studied. Specifically, we generated EEG data with different noise powers according to Eq. (9). Figure 2 shows the spatial mean-square error (MSE), for different signal-to-noise ratios (SNR), computed as follows

$$\text{MSE} = \left( \sqrt{(\hat{x} - x)^2 + (\hat{y} - y)^2 + (\hat{z} - z)^2} \right), \quad (23)$$

where  $(x, y, z)$  are the ground truth coordinates and  $(\hat{x}, \hat{y}, \hat{z})$  are the estimated positions. We observe that, as long as the signal power is higher than the noise power ( $\text{SNR} > 0$  dB), the MSE converges close to zero steady state error. MSE degrades for EEG corrupted with severe noise ( $\text{SNR} \leq 0$  dB).

#### B. Multi-Core BPF versus Single-Core BPF and Full PF

In order to validate the Multi-core BPF, we compare it with the two alternative techniques, single-core BPF and the full PF, from which the proposed method originated. The experiments were performed with the following control conditions: the neural activity from a-pair of correlated dipole sources with 95% ( $M = 0.95$ ) and 30% correlation ( $M = 0.3$ ) were simulated as sinusoidal base waves with amplitudes 0.1 and frequencies 3Hz and 5Hz over 0.5 sec. The performance was evaluated at low SNRs (3dB and 8dB). The target dipoles (ground truth) were taken from the predefined grid with the following  $(x, y, z)$  coordinates:  $d_1 : (0.01, 0.075, 0.02)m$  (right frontal cortex) and  $d_2 : (-0.01, -0.075, -0.01)m$  (left

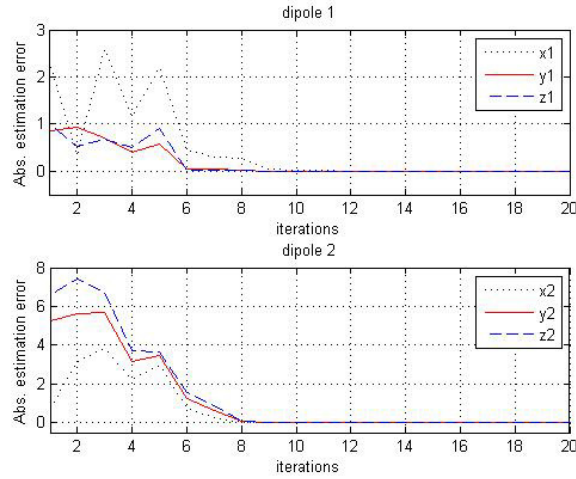


Fig. 3. Absolute estimation error of the dipole locations when the two brain sources are located on the dipole grid and SNR= 3 dB.

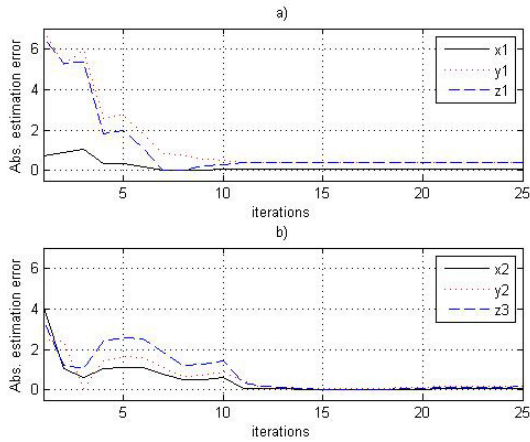


Fig. 4. Absolute estimation error of the dipole locations when only the second brain source coincides with a dipole grid and SNR= 3 dB.

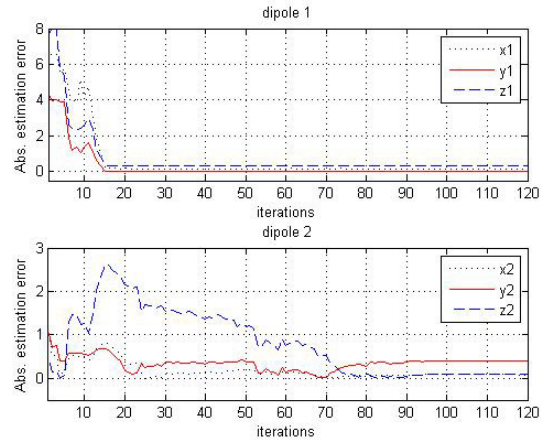


Fig. 5. Absolute estimation error of the dipole locations when none of the brain sources is located on the dipole grid and SNR= 3 dB.

occipital cortex), with a dominant direction of propagation along the  $x$ -axis for  $d_1$  and along the  $y$ -axis for  $d_2$  defined by the following vectors:  $dir_1 : (0.8, 0.1, 0.1)$  and  $dir_2 : (0.1, 0.8, 0.1)$ . The rationale behind this choice is to generate sources located on opposite brain hemispheres; and thus they are spatially distinct but temporally correlated.

First, the effect of the dipole correlation (expressed by  $M$ ) on the beamformer was evaluated (see Figs. 6, 7 and 8). Note that the simulation of dipole correlation changes the sine shape of the base signal. The single-core BF and the multi-core BF provide very similar estimations for uncorrelated dipoles. The higher the correlation level ( $M = 0.95$ ), the more biased are the estimations of the single-core BF as can be seen in Fig. 8. This is due to the filter weight matrix that was computed assuming the source time-courses come from uncorrelated generators.

The results of the spatial location estimation by the three methods are depicted in Figure 10 for  $M = 0.3$  (low correlation) and in Figure 11 for  $M = 0.95$  (high correlation). For low correlation levels (relatively independent sources) the

estimations of the three methods are very similar. The Multi-core BPF clearly outperforms the other methods in the case of highly correlated dipoles. Figure 10 and 11 partially show the volume dipole grid over which the particle filter conducts the search.

Table I summarizes the spatial MSE under varying SNR and varying correlation levels  $M$  for 500 particles, 200 time steps, across 10 Monte Carlo simulations. Even from very noisy EEG data (SNR= 3 dB) and without any prior assumption about the true location of the dipoles, the Multi-core BPF provides estimation within 3-5 mm error distance. The single-core BPF can achieve competitive accuracy, but only for dipoles with low or none temporal correlation. The full PF is less sensitive to dipole correlation and noise. The PF estimation error is relatively high, however if the number of the particles is higher (only 500 in the present scenario) it has the potential to recover better the dipole location. However, a significant amount of memory and computational power are needed, especially when the number of estimated dipoles increases.

Figure 9 presents the normalized weights computed over

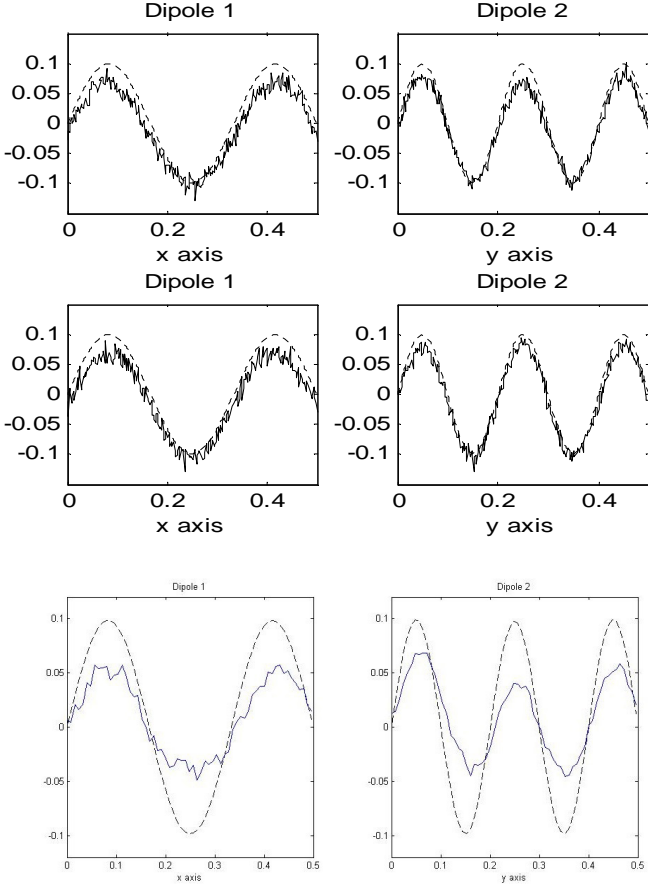


Fig. 6. Source waveform estimation by beamforming for uncorrelated dipoles: the original (dotted line) and the estimated curve (bold line) for dipole 1 (left) and dipole 2 (right) using the Multi-Core BF (top plots), the Single-Core BF (middle plots) and the full PF (bottom plots) with SNR= 3 dB.

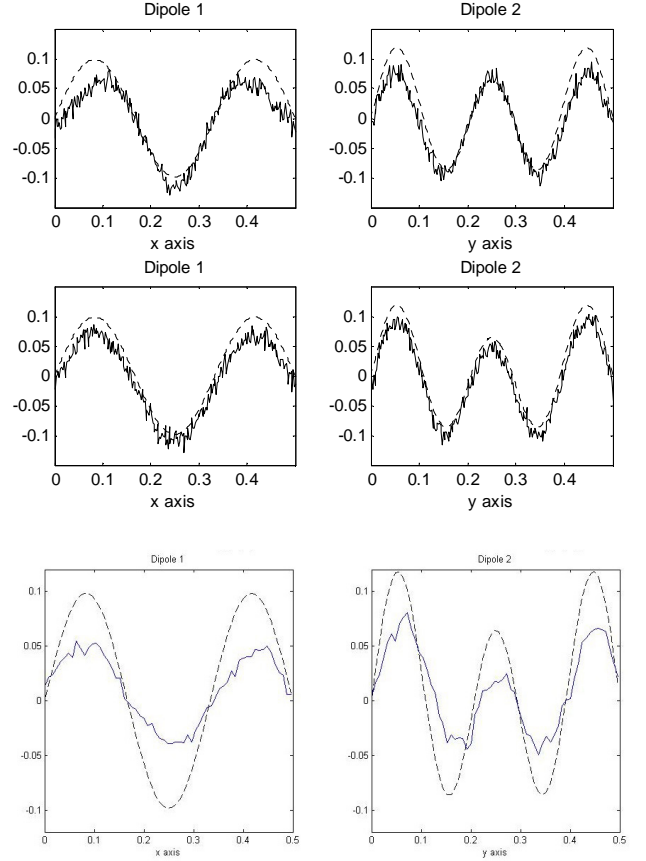


Fig. 7. Source waveform estimation by beamforming for  $M = 0.3$  (low correlation): the original (dotted line) and the estimated curve (bold line) for dipole 1 (left) and dipole 2 (right) using the Multi-Core BF (top plots), the Single-core BF (middle plots) and the full PF (bottom plots) with SNR = 3 dB.

TABLE I  
SPATIAL MEAN SQUARED ERRORS (MSE) IN MILLIMETRES UNDER VARYING SNR AND CORRELATION LEVELS  $M$  FOR  $N = 500$  PARTICLES AND 200 ITERATIONS.

Method	SNR = 3 dB				SNR = 8 dB			
	Dipole 1		Dipole 2		Dipole 1		Dipole 2	
	$M = 0.95$	$M = 0.3$						
Full PF	8.2	8.3	7.3	7.6	6.9	6.7	5.8	5.3
Single-Core BPF	12.2	3.95	9.97	3.3	11.5	3.3	8.7	3.1
Multi-Core BPF	3.4	5.42	1.8	4.41	2.8	4.1	1.5	3.6

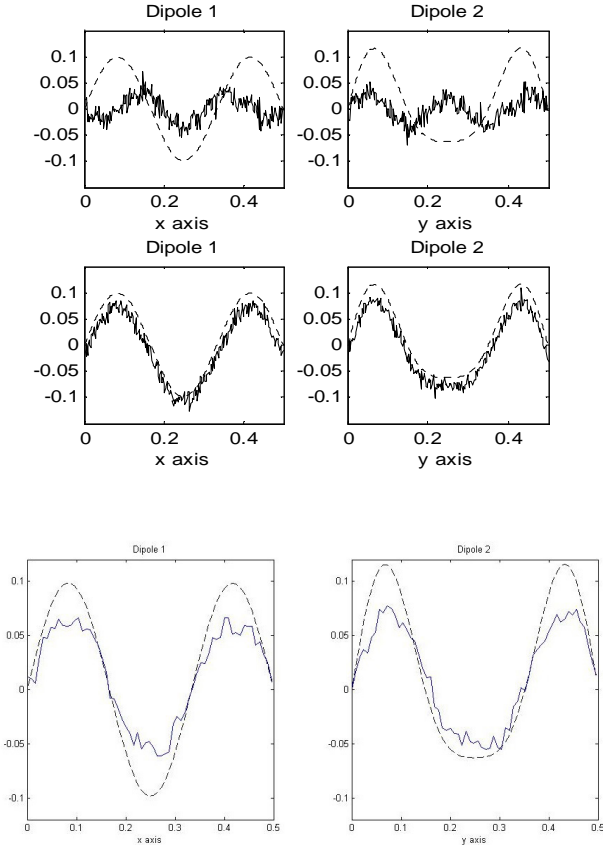


Fig. 8. Source waveform estimation by beamforming for  $M = 0.9$  (high correlation): the original (dotted line) and the estimated curve (bold line) for dipole 1 (left) and dipole 2 (right) using the Multi-Core BF (top plots), the Single-core BF (middle plots) and the full PF (bottom plots) with  $\text{SNR} = 3$  dB.

the recursive PF estimation for some of the iterations  $k$ . Note that based on the current likelihood value at each iteration only few of the particles (from  $N = 500$  particles in total) are pointed out as the most probable candidates for the location of the dipoles. This reduces significantly the computational efforts associated with the exhaustive search over the complete dipole grid conducted by the full beamforming approach or other deterministic parametric methods for brain source localization. In addition, the computational gain of the proposed Beamformer-Particle filter (BPF) is exponential as compared to the full PF. The main computational burden, both in the hybrid approach and in the full PF approach, comes from the PF. The power of the PF in handling nonlinear systems comes at a computational cost. The approximation error of the PF grows exponentially in the dimension of the state vector. It has been shown that the PF collapses unless the number of particles grows super-exponentially in the system dimension [50]. This phenomenon has rendered the PF of limited use in high-dimensional problems. In the proposed BPF approach, the PF estimates the location of the dipoles, whereas the beamformer estimates the dipole waveforms. In the full PF algorithm, both the location and the waveform are estimated using the PF. In particular, the dimension of the state vector

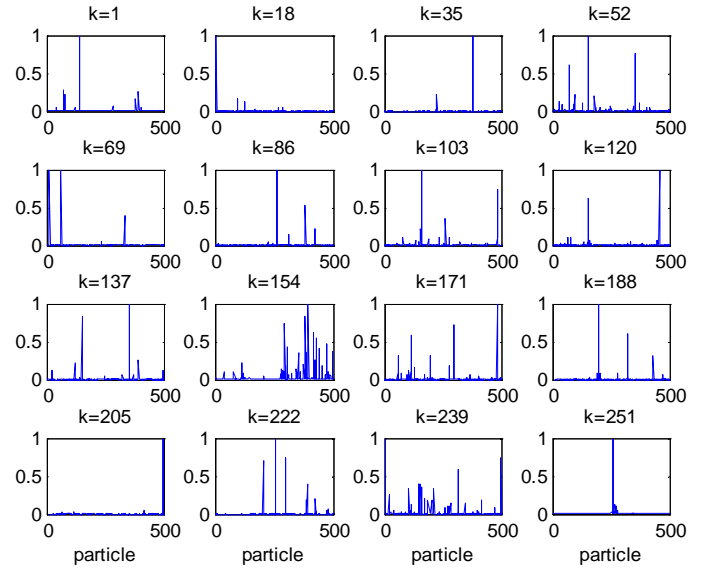


Fig. 9. Normalized weights (Eq. 21) computed over the recursive PF estimation.

in the full PF framework is double the dimension of the state vector in the BPF approach. In our preliminary simulations (not shown here for space limitations), we found that the full PF is able to converge to a near-zero error for one dipole. However, for two or more dipoles, the full PF converges to a non-zero error that increases as the number of dipoles increases (i.e., the number of the state dimension increases). These results are in accordance with the known “curse of dimensionality” issue in Particle Filtering. By reducing the dimension of the state vector that must be estimated by the PF, the proposed Beamformer-PF exponentially reduces the computational burden of the problem.

The computer simulations demonstrate the efficiency of the proposed method for localizing and reconstructing highly correlated sources brain sources from noisy EEG data. A spherical model that approximate the head by three concentric spherical shells representing the brain, skull and scalp is used as in most of the references cited. However, this is a simplification because knowledge of the electrical conductivity map of the head is important since it is known that the solution to the source localization problem is highly dependent on the values taken by the scalp, skull, and brain conductivities [51]. Realistic head modelling of both geometry and anisotropy can

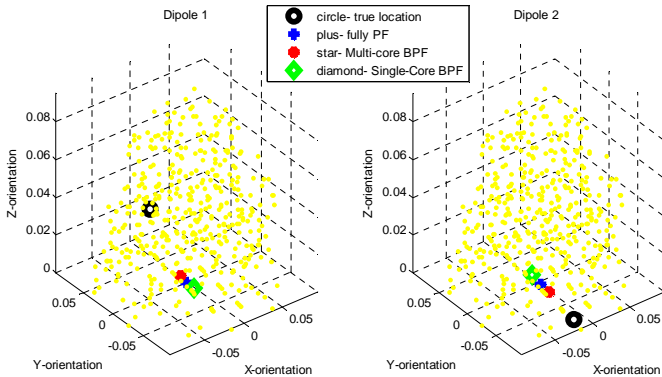


Fig. 10. Spatial location estimates of the dipoles and the ground truth (black) for low correlation,  $M = 0.3$ ,  $\text{SNR} = 3$  dB.

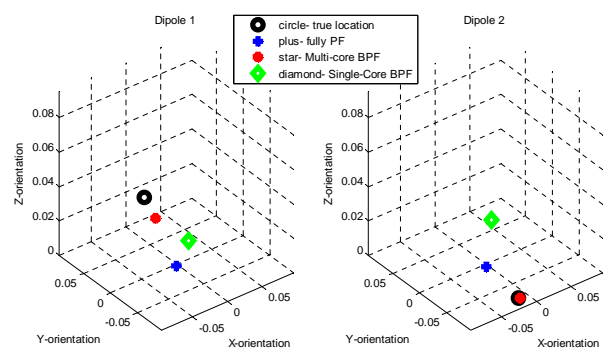


Fig. 11. Spatial location estimates of the dipoles and the ground truth (black) for high correlation,  $M = 0.95$ ,  $\text{SNR} = 3$  dB.

further improve the performance of the beamformer for low SNR.

### C. Results on Real EEG Data

In this section, we demonstrate the estimation accuracy of the proposed algorithm with real EEG data. The data corresponds to Visually Evoked Potential (VEP) signals extracted from thirteen female subjects (20-28 years old). All participants had normal or corrected to normal vision and no history of neurological or psychiatric illness. Different facial expressions (neutral, fearful and disgusted) of 16 individuals (8 males and 8 females) were selected, giving a total of 48 different facial stimuli. Images of 16 different house fronts were superimposed on each of the faces. This resulted in a total of 384 grayscale composite images (9.5 cm wide by 14 cm high) of transparently superimposed face and house.

Participants were seated in a dimly lit room, where a computer screen was placed at a viewing distance of approximately 80 cm coupled to a PC equipped with software for the EEG recording. The images were divided into two experimental blocks. In the first, the participants were required to attend to the houses (ignoring the faces) and in the other they were required to attend to the faces (ignoring the houses). The participants task was to determine, on each trial, if the current house or face (depending on the experimental block) is the same as the one presented on the previous trial. Stimuli were presented in a sequence of 300 ms each and were preceded by a fixation cross displayed for 500 ms. The inter-trial interval was 2000 ms.

EEG signals were recorded from 20 electrodes (Fp1, Fp2, F3, F4, C3, C4, P3, P4, O1, O2; F7, F8, T3, T6; P7, P8, Fz, Cz, Pz, Oz) according to the 10/20 International system. Electrooculogram (EOG) signals were also recorded from electrodes placed just above the left supra orbital ridge (vertical EOG) and on the left outer canthus (horizontal EOG). VEP were calculated off-line averaging segments of 400 points of digitized EEG (12 bit A/D converter, sampling rate 250 Hz). These segments covered 1600 ms comprising a pre-stimulus interval of 148 ms (37 samples) and post-stimulus onset

interval of 1452 ms. The EEG signal was visually inspected, prior to processing, and those segments with excessive EOG artifacts were manually eliminated (see Fig. 12 where epoch 2 was manually discarded). Only trials with correct responses were included in the data set. The experimental setup was designed by Santos *et al.* [52] for their study on subject attention and perception using VEP signals.

Figure 13 represents 18 trials of four channels enhanced by Principal Component Analysis (PCA). In the reconstructed signals, it is possible to identify a positive peak in the range of 100 - 160 ms, known as P100. P100 corresponds to the perception of the sensory stimulus, a brain activity that is known to happen in the primary visual cortex. The occipital channels (O1, Oz) that measure the brain activity around the visual cortex present the largest peak. We apply the proposed beamforming particle filter to estimate the two strongest sources ( $d_1$  and  $d_2$ ) that may have produced the P100 peak. The results of the estimation are summarized in Figs. 14 and 15. The dipole reconstruction from real EEG data took more iterations than with synthetic data, about 1300 iterations for dipole 1 and 480 iterations for dipole 2. After that the PF weights converged to fixed values and therefore the identified spatial coordinates reached steady states. It is very interesting to observe that the final coordinates of  $d_1 : (0.71\text{mm}, -6.3\text{mm}, -1.9\text{mm})$  and  $d_2 : (6.8\text{mm}, -2\text{mm}, -6.14\text{mm})$  correspond to the zone of the primary visual cortex as illustrated in Fig. 16. Therefore, the proposed beamformer-based PF successfully estimated the space coordinates of the two strongest brain sources, producing the P100 peak, as located in the zone of the primary visual cortex.

## VII. CONCLUSIONS

This paper proposes a multi-core Beamformer Particle Filter (multi-core BPF) for solving the ill-posed EEG inverse problem. The method combines a particle filter (statistical approach) for estimation of the spatial location and a multi-core beamformer (deterministic approach) for estimation of temporally correlated dipole waveforms in a recursive framework. As a result the estimation accuracy is

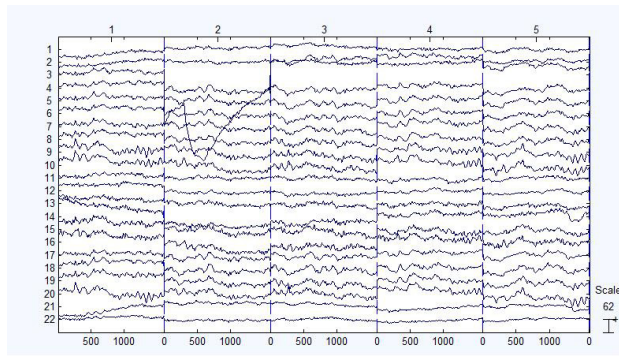


Fig. 12. EEG signals (channels 1-20) and EOG signals (channels 21-22). Horizontal axis [ms], vertical axis [EEG channels].

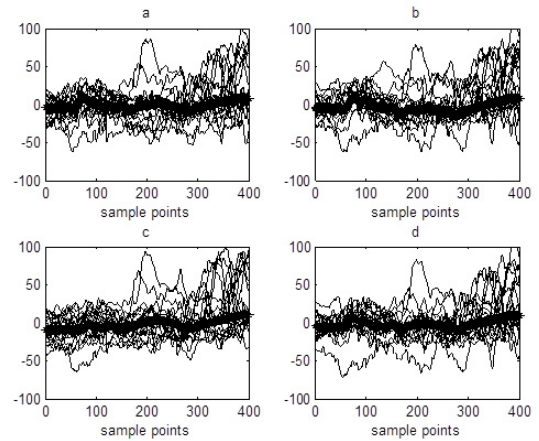


Fig. 13. Superposition of 18 PCA enhanced Visually Evoked Potentials (VEP) recorded by four electrodes: a) O1; b) O2; c) Pz; d) Oz. The bold trace represents the average of all trials used to test the particle filter.

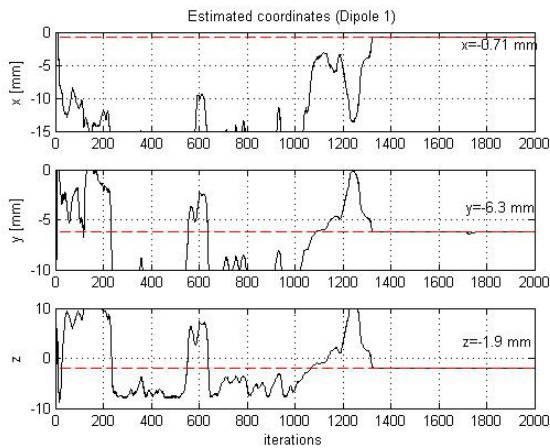


Fig. 14. Estimation of the source location (Dipole 1) that produced the P100 peak.

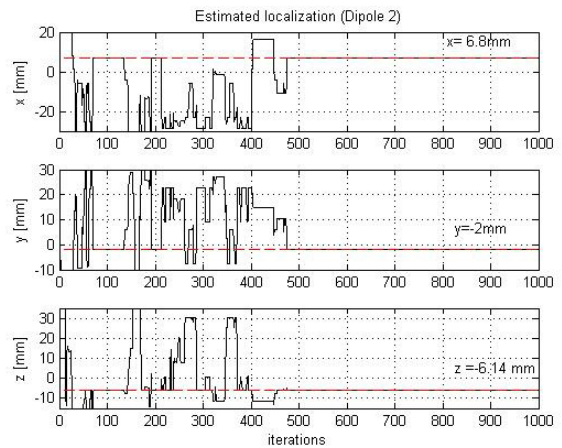


Fig. 15. Estimation of the source location (Dipole 2) that produced the P100 peak.

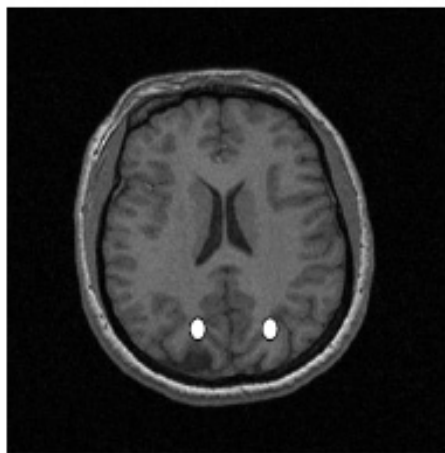


Fig. 16. Primary visual cortex: axial view. The estimated active zones are depicted in white circles.

improved. This general framework comprising the multi-core BF allows to cope with the main challenges of the EEG brain source recovering with particular emphases upon temporally correlated dipoles. We conducted extensive simulations, based on generated and real EEG experiments, in order to study the accuracy and robustness of the proposed algorithm. The multi-core BPF guarantees convergence to the correct spatial-temporal source coordinates as long as the power of the signal is higher than the power of the noise within the EEG measurements. We have also conducted EEG experiments where subjects were exposed to visual stimuli. The multi-core BPF localized the two strongest brain sources that have produced the recorded EEG signal within the expected visual cortex zone. Numerous challenges still remain for an objective assessment of the relative performance of inverse algorithms and the statistical significance of different solutions computed from simulated and experimental data. Additional research efforts are needed to come up with a real-time solution of the inverse problem. Our recent ongoing work suggests that

the proposed methodology can be transferred from the “fixed dipoles” case (as in the present work) to the “moving dipoles” case with encouraging results.

**Acknowledgments.** We are grateful to the support of the Operational Program Competitiveness Factors - Compete and by National Funds through FCT - Foundation for Science and Technology in the context of the project FCOMP-01-0124-FEDER-022682 (FCT reference PEst-C/EEI/UI0127/2011) and the UK Engineering and Physical Sciences Research Council (EPSRC) for the support via the Bayesian Tracking and Reasoning over Time (BTaRoT) grant EP/K021516/1. This project is also supported by Award Number R01GM096191 from the USA National Institute Of General Medical Sciences (NIH/NIGMS). The authors would like to extend their gratitude to Mr. Bradley Ebinger, a graduate student with the Department of Electrical and Computer Engineering at Rowan University, for his contribution to the implementation of some of the code.

## REFERENCES

- [1] S. Sanei and J. Chambers, *EEG Signal Processing*. John Wiley & Sons, 2007.
- [2] A. Galka, O. Yamashita, T. Ozaki, R. Biscay, and P. Valds-Sosa, “A solution to the dynamical inverse problem of EEG generation using spatiotemporal Kalman filtering,” *Neuroimage*, vol. 23, no. 2, pp. 435–453, 2004.
- [3] B. Kamousi, Z. Liu, and B. He, “An EEG inverse solution based brain-computer interface,” *The International Journal of Bioelectromagnetism*, vol. 7, no. 2, pp. 292–294, 2005.
- [4] L. Qin, L. Ding, and B. He, “Motor imagery classification by means of source analysis for brain computer interface applications,” *Journal of Neural Engineering*, vol. 2, no. 4, pp. 65–72, Dec. 2005.
- [5] Q. Noirhomme, R. Kitney, and B. Macq, “Single-trial EEG source reconstruction for brain-computer interface,” *IEEE Transactions on Biomedical Engineering*, vol. 55, no. 5, pp. 1592–1601, May 2008.
- [6] M. Grosse-Wentrup, C. Liefhold, K. Gramann, and M. Buss, “Beamforming in non-invasive brain-computer interfaces,” *IEEE Transactions on Biomedical Engineering*, vol. 56, no. 4, pp. 1209–1219, April 2009.
- [7] S. Baillet, J. Mosher, and R. Leahy, “Electromagnetic brain mapping,” *IEEE Signal Processing Magazine*, vol. 18, no. 6, pp. 14–30, November 2001.
- [8] C. Michel, M. Murray, G. Lantz, S. Gonzalez, L. Spinelli, and R. G. de Peralta, “EEG source imaging,” *Clinical Neurophysiology*, vol. 115, no. 10, pp. 2195–222, October 2004.
- [9] J. Gross and A. Ioannides, “Linear transformations of data space in meg,” *Physics in Medicine and Biology*, vol. 44, no. 8, pp. 2081–2097, August 1999.
- [10] B. V. Veen, W. V. Dronghen, M. Yuchtman, and A. Suzuki, “Localization of brain electrical activity via linearly constrained minimum variance spatial filter,” *IEEE Transactions on Biomedical Engineering*, vol. 44, no. 9, pp. 867–880, September 1997.
- [11] A. Cichocki and S. Amari, *Adaptive Blind Signal and Image Processing: Learning Algorithms and Applications*. John Wiley & Sons, July 2002.
- [12] A. Hyvärinen, J. Karhunen, and E. Oja, *Independent Component Analysis*. John Wiley & Sons, 2001.
- [13] S. J. Kiebel, J. Daunizeau, C. Phillips, and K. J. Friston, “Variational bayesian inversion of the equivalent current dipole model in EEG/MEG,” *NeuroImage*, vol. 39, no. 2, pp. 728–741, January 2008.
- [14] A. Sorrentino, L. Parkkonen, and M. Piana, “Particle filters: A new method for reconstructing multiple current dipoles from MEG data,” in *International Congress Series*, vol. 1300, 2007, pp. 173–176.
- [15] A. Sorrentino, L. Parkkonen, A. Pascarella, C. Campi, and M. Piana, “Dynamical MEG source modeling with multi-target bayesian filtering,” *Human Brain Mapping*, vol. 30, no. 6, pp. 1911–1921, June 2009.
- [16] M. Arulampalam, S. Maskell, N. Gordon, and T. Clapp, “A tutorial on particle filters for online nonlinear/non-gaussian bayesian tracking,” *IEEE Transactions on Signal Processing*, vol. 50, no. 2, pp. 174–188, February 2002.
- [17] A. Doucet and A. M. Johansen, “A tutorial on particle filtering and smoothing: Fifteen years later,” *Handbook of Nonlinear Filtering*, vol. 12, pp. 656–704, 2009.
- [18] F. Gustafsson, “Particle filter theory and practice with positioning applications,” *IEEE Transactions on Aerospace and Electronics Systems Magazine Part II: Tutorials*, vol. 25, no. 7, pp. 53–82, 2010.
- [19] L. Mihaylova, A. Y. Carmi, F. Septier, A. Gning, S. K. Pang, and S. Godsill, “Overview of Bayesian sequential Monte Carlo methods for group and extended object tracking,” *Digital Signal Processing*, vol. 25, no. 1, pp. 1–16, 2014.
- [20] O. Cappé, S. Godsill, and E. Mouline, “An overview of existing methods and recent advances in sequential Monte Carlo,” *IEEE Proceedings*, vol. 95, no. 5, pp. 899–924, 2007.
- [21] J. Antelis and J. Minguez, “Dynamic solution to the EEG source localization problem using kalman filters and particle filters,” in *Proceedings of the International Conference of the IEEE Engineering in Medicine and Biology Society*, 2009, pp. 77–80.
- [22] H. Mohseni, E. Wilding, and S. Sanei, “Sequential Monte Carlo techniques for eeg dipole placing and tracking,” in *Proceedings from the 5th IEEE Sensor Array and Multichannel Signal Processing Workshop*, July 2008, pp. 95–98.
- [23] L. Miao, J. Zhang, C. Chakrabarti, and A. Papandreou-Suppappola, “Efficient bayesian tracking of multiple sources of neural activity: Algorithms and real-time FPGA implementation,” *IEEE Transactions on Signal Processing*, vol. 61, no. 3, pp. 633–647, Feb 2013.
- [24] K. Sekihara, S. Nagarajan, D. Poeppel, A. Marantz, and Y. Miyashita, “Reconstructing spatio-temporal activities of neural sources using an meg vector beamformer technique,” *IEEE Transactions on Biomedical Engineering*, vol. 48, no. 7, pp. 760–771, July 2001.
- [25] M. Brookes, C. Stevenson, G. Barnes, A. Hillebrand, M. Simpson, S. Francis, and P. Morris, “Beamformer reconstruction of correlated sources using a modified source model,” *Neuroimage*, vol. 34, pp. 1454–1465, 2007.
- [26] M. Diwakar, M.-X. Huang, R. Srinivasan, D. Harrington, A. Robb, A. Angeles, L. Muzzatti, R. Pakdaman, T. Song, R. Theilmann, and R. Lee, “Dual-core beamformer for obtaining highly correlated neural networks in MEG,” *Neuroimage*, vol. 54, pp. 253–263, 2011.
- [27] S. Dalal, K. Sekihara, and S. S. Nagarajan, “Modified beamformers for coherent source region suppression,” *IEEE Transactions on Biomedical Engineering*, vol. 53, no. 7, pp. 1357–1363, 2006.
- [28] M. Popescu, E. Popescu, T. Chan, S. Blunt, and J. D. Lewine, “Spatio-temporal reconstruction of bilateral auditory steady-state responses using MEG beamformers,” *IEEE Transactions on Biomedical Engineering*, vol. 55, no. 3, pp. 1092–1102, 2008.
- [29] J. Mosher and R. Leahy, “Recursive music: a framework for EEG and MEG source localization,” *IEEE Transactions on Biomedical Engineering*, vol. 45, no. 11, pp. 1342–1354, November 1998.
- [30] N. J. Gordon, D. J. Salmond, and A. F. M. Smith, “Novel approach to nonlinear/non-Gaussian Bayesian state estimation,” *IEE Proceedings*, vol. 140, no. 2, pp. 107–113, April 1993.
- [31] A. Doucet, N. Freitas, and E. N. Gordon, *Sequential Monte Carlo Methods in Practice*. New York: Springer-Verlag, 2001.
- [32] S. Haykin, *Adaptive Filter Theory*, 4th ed. Prentice Hall, 2001.
- [33] Y. Salu, L. Cohen, D. Rose, S. Sato, C. Kufita, and M. Hallet, “An improved method for localizing electric brain dipoles,” *IEEE Transactions on Biomedical Engineering*, vol. 37, no. 7, pp. 699–705, July 1990.
- [34] B. Anderson and J. Moore, *Optimal Filtering*. Dover Publications, 2005.
- [35] B. Ristic, S. Arulampalam, and N. Gordon, *Beyond the Kalman Filter: Particle Filters for Tracking Applications*. Boston, London: Artech House, 2004.
- [36] T. R. Knösche, E. M. Berends, H. R. Jagers, and M. J. Peters, “Determining the number of independent sources of the EEG: a simulation study on information criteria,” *Brain Topography*, vol. 11, no. 2, pp. 111–124, 1998.
- [37] S. Robinson and J. Vrba, “Functional neuroimaging by syntheticaperture magnetometry (SAM),” in *Recent Advances in Biomagnetism*, T. Yoshimoto, M. Kotani, S. Kuriki, H. Karibe, and N. Nakasato, Eds. Tohoku University Press, Sendai, Japan, 1999, pp. 302–305.
- [38] A. Hillebrand and G. Barnes, “The use of anatomical constraints with MEG beamformers,” *Neuroimage*, vol. 20, no. 4, pp. 2302–2313, 2003.
- [39] M. Huang, J. Shih, R. Lee, D. Harrington, R. Thoma, M. Weisend, F. Hanion, K. Paulson, T. Li, K. Martin, G. Miller, and J. Canive, “Commonalities and differences among vectorized beamformers in electromagnetic source imaging,” *Brain Topography*, vol. 16, no. 3, pp. 139–158, 2004.
- [40] C. Chen, A. Pogosyan, L. Zrinzo, S. Tisch, P. Limousin, K. Ashkan, T. Youstry, M. Hariz, and P. Brown, “Intra-operative recordings of local field potentials can help localize the subthalamic nucleus in Parkinson’s disease surgery,” *Exp. Neurology*, pp. 214–221, 2006.
- [41] A. Herdman, A. Wollbrink, W. Chan, R. Ishii, B. Ross, and C. Pantev, “Determination of activation areas in the human auditory cortex by

- means of synthetic aperture magnetometry," *Neuroimage*, vol. 20, no. 2, pp. 995–1005, 2003.
- [42] D. Cheyne, A. Bostan, W. Gaetz, and E. Pang, "Event-related beamforming: a robust method for presurgical functional mapping using meg," *Clinical Neurophysiology*, vol. 118, no. 8, pp. 1691–1704, 2007.
- [43] H. Yuan, A. Doud, A. Gururajan, and B. He, "Cortical imaging of event-related (de)synchronization during online control of brain-computer interface using minimum-norm estimates in frequency domain," *IEEE Transactions on Neural Systems and Rehabilitation Engineering*, vol. 16, no. 5, pp. 425–431, Oct 2008.
- [44] J. Vrba and S. E. Robinson, "Signal processing in magnetoencephalography," *Methods*, vol. 25, no. 2, pp. 249 – 271, 2001.
- [45] E. Gysels, P. Renevey, and P. Celka, "Svm-based recursive feature elimination to compare phase synchronization computed from broadband and narrowband EEG signals in braincomputer interfaces," *Signal Processing*, vol. 85, no. 11, pp. 2178 – 2189, 2005, neuronal Coordination in the Brain: A Signal Processing Perspective.
- [46] Y. Lai, W. V. Drongelen, L. Ding, K. Hecox, V. Towle, D. Frim, and B. He, "Estimation of in vivo human brain-skull conductivity ratio from simultaneous extra and intra-cranial electrical potential recordings," *Clinical Neurophysiology*, vol. 116, no. 2, pp. 456–465, February 2005.
- [47] H. Yuan, T. Liu, R. Szarkowski, C. R. J. Ashe, and B. He, "An EEG and fMRI study of motor imagery: negative correlation of bold and eeg activity in primary motor cortex," *Neuroimage*, vol. 49, pp. 2596–2606, 2010.
- [48] O. Gilad, L. Horesh, and D. Holder, "Design of electrodes and current limits for low frequency electrical impedance tomography of the brain," *Medical & Biomedical Engineering & Comput.*
- [49] J. Gross, J. Kujala, M. Hamalainen, L. Timmermann, A. Schnitzler, and R. Salmelin, "Dynamic imaging of coherent sources: studying neural interactions in the human brain," *Proceedings of the National Academy of Sciences*, vol. 98, no. 2, pp. 694–699, 2001.
- [50] T. Bengtsson, P. Bickel, and B. Li, "Curse-of-dimensionality revisited: Collapse of the particle filter in very large scale systems," *Probability and Statistics: Essays in Honor of David A. Freedman*, p. 316334, 2008.
- [51] S. Goncalves, J. de Munck, J. Verbunt, and F. Bijma, "In vivo measurement of the brain and skull resistivities using an eit-based method and realistic models for the head," *IEEE Transactions on Biomedical Engineering*, vol. 50, no. 6, pp. 754 – 767, 2003 2003.
- [52] I. Santos, J. Iglesias, E. I. Olivares, and A. Young, "Differential effects of object-based attention on evoked potentials to fearful and disgusted faces," *Neuropsychologia*, vol. 46, no. 5, pp. 1468–1479, 2008.